Iran. J. Radiat. Res., 2012; 10 (3-4): 183-186

Megavoltage dose enhancement of gold nanoparticles for different geometric set-ups: Measurements and Monte Carlo simulation

S.H. Mousavie Anijdan[1,2], A. Shirazi[1], S.R. Mahdavi[1*], A. Ezzati[3], B. Mofid[4], S. Khoei[1], M.A. Zarrinfard[5]

[1]Department of Medical Physics and Engineering, School of Medicine, Tehran University of Medical Sciences, Tehran, Iran
[2]Department of Medical Physics, Babol University of Medical Sciences, Babol, Iran
[3]Department of Energy Engineering, Sharif University of Technology, Tehran, Iran
[4]Department of Radiation Oncology, Shahid Beheshti University of Medical Sciences, Tehran, Iran
[5]Department of Medical Nanotechnology, Faculty of Advanced Medical Sciences, Tehran, Iran

Background: Gold nanoparticles (GNPs) have been shown as a good radiosensitizer. In combination with radiotherapy, several studies with orthovoltage X-rays have shown considerable dose enhancement effects. This paper reports the dose enhancement factor (DEF) due to GNPs in 18 megavoltage (MV) beams. ***Materials and Methods:*** Different geometrical 50-nm GNPs configurations at a concentration of 5 mg/ml were used by both experimental and Monte Carlo (MC) simulation in a deep-seated tumor-like insertion within a phantom. Using MCNP repeated structure capability; a large number of gold nanospheres with a semi-random distribution were applied to simulate this phantom based study. Thermoluminescence dosimetries were used to verify the process of irradiation and MC simulation. ***Results:*** Under geometries with different probable combinations of water and GNPs distribution in the tumor, the percentage depth dose and DEF were calculated. Incorporation of GNPs into the radiation field in our set-ups showed a 12% DEF. ***Conclusion:*** We show that the method of nanoparticles, distribution, and orientation can effectively change the DEF value.
Iran. J. Radiat. Res., 2012; 10(3-4): 183-186

Keywords: *Monte Carlo simulation, gold nanoparticles (GNPs), dose enhancement.*

INTRODUCTION

The basic principle of radiotherapy is to deliver maximum doses to the tumor while protecting the normal structures as much as possible. The dose enhancement in target is a technique that needs radiosensitizer with high atomic number elements and has been proposed in various studies [1-3]. Several simulation studies have shown sensitization with kilovoltage radiation therapy. Most of these studies were performed with energies near the K-edge of gold [4, 5]. The limited penetration of kV X-rays is the greatest challenge of radiotherapy in comparison to MV. However, the effective radiosensitization depends on factors such as energy of photon, GNPs size, concentration, and the location within the cell. *In-vitro* and animal studies have also shown that GNPs can enhance the radiobiological effect of radiation dose [6-8].

Simulations have reported a DEF of ~2 times with a 0.5-1% radiosensitizer per weight at energies of 80-140 kVp (5). All MC simulations are typically based on two calculation methods. Most simulate mixture of gold as a percentage weight of medium, a model known as gold-water mixture [1-4].

Another method simulates a large number of GNPs in nanometer-scale geometry, known as gold nanospheres solution [9]. The purpose of this study was to demonstrate dosimetrically, whether GNRT is feasible for the treatment of deep tumors in clinically relevant MV energy with different geometrical GNPs distributions.

MATERIALS AND METHODS

The DEF was estimated in according to the following definition: the ratio of the average deposited dose to the volume both

Corresponding author:
Dr. Seied Rabi Mahdavi,
Department of Medical Physics and Engineering, School of Medicine, Tehran University of Medical Sciences, Tehran, Iran.
Fax: *+98 21 88622647*
E-mail: *srmahdavi@hotmail.com*

with and without the presence of GNPs after a definitive irradiation [1-2].

A 15 × 15 × 15 cm^3 Plexiglass phantom was made of two separate slabs. An upper slab with a thickness of 10 cm is thick enough to produce transient charged particle equilibrium and scatter condition. The lower slab with a 5 cm thickness has a hollow like cavity for placing two separated plexiglass cylinders with a 2 cm diameter and 1 cm height. The phantom was scanned by CT and images were transferred to a planning system. The dosimetric planning was done so a uniform dose of 100 cGy would be delivered to the volume, which was situated between the two cylinders at 131 cm from the source.

Dosimetry was done with GR100M, PTW Freiburg chips. TLDs calibration was done by Cobalt-60 beam. The TLDs were then packed within a thin layer of plastic to prevent the loss of function, and they were placed in three or four levels at 130, 131, 132, and 132.6 cm from the source in the tumor-like insert phantom. The GNPs were provided from plasmachem GmbH at 50 nm with a 5 mg/ml and all of the measurements were performed with this single concentration. The 18 MV beams were provided by the Varian 2100 C/D LINAC. A 5 × 5 cm2 field was opened on the cerrobend block as it confined treatment field into a circle with 3.6 cm diameter in the center of tumor phantom. DEFs were calculated from transmitted radiation dose for each different geometric set-up.

The MCNP4C code was used for calculating DEF. The semi-random distribution of the GNPs was simulated by using MC repeated structure capability. The cubic size was chosen so that the GNPs density would be at 5 mg/ml. The cube was then filled into the tumor area. The LINAC head was simulated by using open literature information for 18 MV photons. The circular field was used with a tumor assumed to be a cylindrical volume. The model included the target, flattening filter, primary, and a secondary collimator. Simulations were done even to obtaining less than 1.6% relative error in the tumor-like insert area. We used energy deposition tally (*f8). The number of histories for each simulation was 2.1 × 109.

RESULTS

Figure 1 shows the results of the calibration measurements. The linear behavior of this curve depicts the precision of TLDs in estimating the absorbed dose in a wide range of exposures. The DEF value in different levels (or points) for this tumor-like phantom is estimated by differences of the PDD value at different points of A, B, C and D in the tumor phantom. The results of DEF measurements at levels B, C, and D were calculated as 8.33%, 1.8% and 2.8%, respectively.

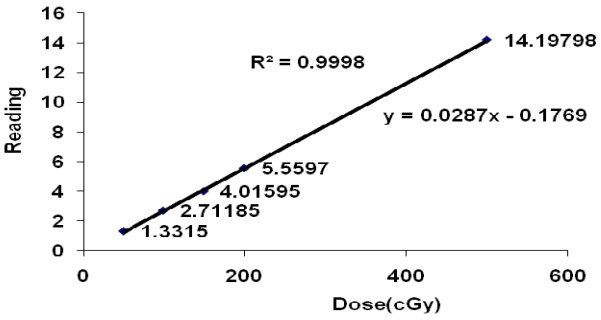

Figure 1. Reading of TLD- GR 100 M measured in air (the calibration curve).

A number of simulations were performed to calculate PDD and DEF within the tumor -like insert. Figure 2 shows that the maximum DEF is about 12% when two parts of tumor phantom are filled with GNPs. The maximum DEF for each case depends on the volume of GNPs and geometric set-ups of the system. To obtain a uniform dose distribution in the tumor volume by MCNP, a high SSD had to be selected. The peak of DEF was moved about 3-5 mm after level B and about 3-5 mm after level C in the case that the GNPs are in upper and the lower part is filled with water.

DISCUSSION

This study further confirms the

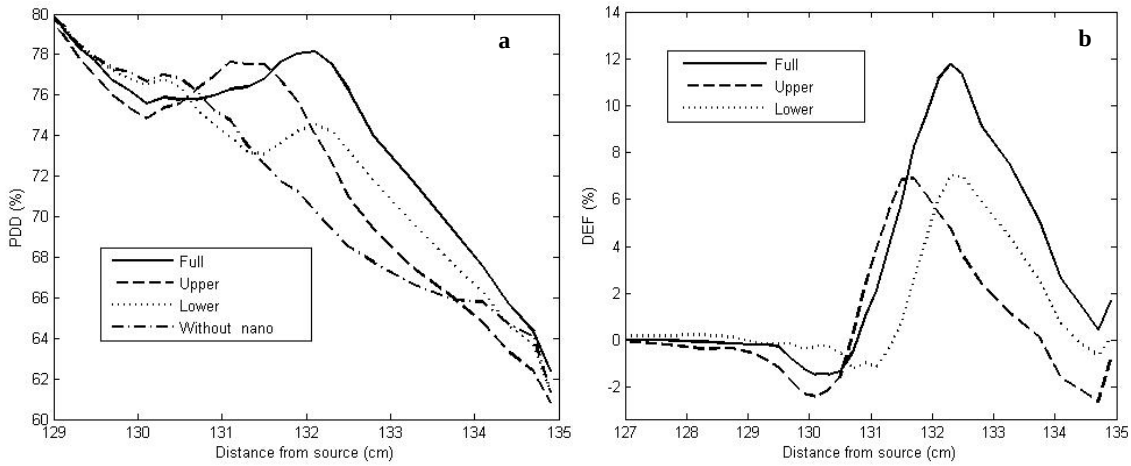

Figure 2. MC simulation. **a)** calculated PDD and beam attenuation, and **b)** DEF values estimated from PDDs for different geometric set-ups.

simulation results under the different geometric conditions mentioned by other author [10-12].

For higher photon energies, Compton and pair production processes are major competing mechanisms. The subsequent secondary electrons from each process may have different energies and ranges of motion. The average range of energetic photoelectrons and Compton electrons might be from a few to several hundred microns, respectively [5]. When only photoelectric interaction is considered, the range of electrons escaping from 100-nm GNPs after irradiation with 6 MV is about 81 µm [4]. Also Zhang *et al.* calculated this range as about 85 µm when the photon energy was 380 keV and photoelectric interaction only [9]. If both photoelectric and Compton processes are encountered, the average range of secondary electrons would be 1090 µm for the same condition [13].

For 18 MV beam the pair production process in the high-Z element efficiently converts the photon energy to the energy of the secondary electrons/positrons, which travel on the order of several millimeters (about 2 MeV/10 mm). Simulation of DEF versus SSD (figure 2b) shows that the maximum DEF occurs at 6–10 mm from bottom of GNPs container. The reason for shifting of the dose enhancement peak to the right side on the graph can be due to the range of the secondary particles raised from the lower end of the GNPs container [14].

Roeske *et al.* reported a 0.5 - 0.8% DEF for 18 MV in comparison to the 6 MV beams, which can be due to the presence of pair production interaction [15]. These results are apparently much lower than our findings. Other simulations have also been used in MV [16]. They found a DEF less than 5% with 6-24 MV flattened beams at 20-30 mg/ml concentration of gadolinium. When the investigators removed the flattening filter from the LINAC, the DEFs were changed to 8.4-23.1% for 18-2 MV beams. Cho estimated the DEF for various geometric set-ups of different GNPs concentrations, at gamma rays, KV and MV photon by MC methods (1). They also found a less than 5% DEF at 18 MV with a relatively high concentration (20-30 mg/ml) of radiosensitization, which is lower than our results (8-12%) with a 5 mg/ml concentration. It seems that the DEF value strongly depends on the position and geometry of the GNPs distribution with respect to the tumor volume.

The integrating mechanism to explain DEF in MV range recently has also been discussed by different researches from the point of radiobiological matter. It has been revealed that the Local Effect Model can be a model of choice to predict biological effect of nanoparticle dose enhancement [17]. This model originally applied to calculate dose

inhomogeneities along heavy ion tracks. Correlating the biologically dose enhancement to the underlying physical mechanism is an open subject for further investigation. Nano and microdosimetric studies may be able to explain the ultra structural damage at the cellular level [18].

REFERENCES

1. Cho SH (2005) Estimation of tumour dose enhancement due to gold nanoparticles during typical radiation treatments: a preliminary Monte Carlo study. *Phys Med Biol,* ***50:*** *N163-N173.*
2. Cho SH, Jones BL, Krishnan S (2009) The dosimetric feasibility of gold nanoparticle-aided radiation therapy (GNRT) via brachytherapy using low-energy gamma-/X-ray sources. *Phys Med Biol,* ***54:*** *4889-4905.*
3. McMahon SJ, Mendenhall MH, Jain S, Currell F (2008) Radiotherapy in the presence of contrast agents: a general figure of merit and its application to gold nanoparticles. *Phys Med Biol,* ***53:*** *5635-5651.*
4. Lechtman E, Chattopadhyay N, Cai Z, Mashouf S, Reilly R, Pignol JP (2011) Implications on clinical scenario of gold nanoparticle radiosensitization in regards to photon energy, nanoparticle size, concentration and location. *Phys Med Biol,* ***56:*** *4631-4647.*
5. Hainfeld JF, Dilmanian FA, Slatkin DN, Smilowitz HM (2008) Radiotherapy enhancement with gold nanoparticles. *J Pharm Pharmacol,* ***60:*** *977-985.*
6. Hainfeld JF, Slatkin DN, Smilowitz HM (2004) The use of gold nanoparticles to enhance radiotherapy in mice. *Phys Med Biol,* ***49:*** *N309-N315.*
7. Chithrani BD, Ghazani AA, Chan WCW (2006) Determining the size and shape dependence of gold nanoparticle uptake into mammalian cells. *Nano Lett,* ***6:*** *662-668.*
8. Roa W, Zhang X, Guo L, Shaw A, Hu X, Xiong Y, Gulavita S, Patel S, Sun X, Chen J, Moore R, Xing JZ (2009) Gold nanoparticle sensitize radiotherapy of prostate cancer cells by regulation of the cell cycle. *Nanotechnology,* ***20:*** *375101-375110.*
9. Zhang SX, Gao J, Buchholz TA, Wang Z, Salehpour MR, Drezek RA, Yu TK (2009) Quantifying tumor-selective radiation dose enhancements using gold nanoparticles: a monte carlo simulation study. *Biomed Microdevices,* ***11:*** *925-933.*
10. Verhaegen F, Reniers B, Deblois F, Devic S, Seuntjens J, Hristov D (2005) Dosimetric and microdosimetric study of contrast-enhanced radiotherapy with kilovolt X-rays. *Phys Med Biol,* ***50:*** *3555-3569.*
11. Morris KN, Weil MD, Malzbender R (2006) Radiochromic film dosimetry of contrast-enhanced radiotherapy (CERT). *Phys Med Biol,* ***51:*** *5915-5925.*
12. Rahman WN, Wong CJ, Yagi N, Davidson R, Geso M (2010) Dosimetry and its enhancement using gold nanoparticles in synchrotron based microbeam and stereotactic radiosurgery. *Aip Conf Proc,* ***1266:*** *107-110.*
13. Leung MK, Chow JC, Chithrani BD, Lee MJ, Oms B, Jaffray DA (2011) Irradiation of gold nanoparticles by X-rays: Monte Carlo simulation of dose enhancements and the spatial properties of the secondary electrons production. *Med Phys,* ***38:*** *624-631.*
14. Alkhatib A, Watanabe Y, Broadhurst JH (2009) The local enhancement of radiation dose from photons of MeV energies obtained by introducing materials of high atomic number into the treatment region. *Med Phys,* ***36:*** *3543-3548.*
15. Roeske JC, Nunez L, Hoggarth M, Labay E, Weichselbaum RR (2007) Characterization of the theorectical radiation dose enhancement from nanoparticles. *Technol Cancer Res Treat,* ***6:*** *395-402.*
16. Robar JL (2006) Generation and modelling of megavoltage photon beams for contrast-enhanced radiation therapy. *Phys Med Biol,* ***51:*** *5487-5504.*
17. McMahon SJ, Hyland WB, Muir MF, Coulter JA, Jain S, Butterworth KT, Schettino G, Dickson GR, Hounsell AR, O'Sullivan JM, Prise KM, Hirst DG, Currell FJ (2011) Biological consequences of nanoscale energy deposition near irradiated heavy atom nanoparticles. *Sci Rep-Uk,* ***1:*** *1-9.*
18. McMahon SJ, Hyland WB, Muir MF, Coulter JA, Jain S, Butterworth KT, Schettino G, Dickson GR, Hounsell AR, O'Sullivan JM, Prise KM, Hirst DG, Currell FJ (2011) Nanodosimetric effects of gold nanoparticles in megavoltage radiationtherapy. *Radiother Oncol,* ***100:*** *412-416.*